Molecular Vision 2015; 21:360-377 <http://www.molvis.org/molvis/v21/360>
Received 6 October 2014 | Accepted 7 April 2015 | Published 9 April 2015

Regulation of the hyperosmotic induction of aquaporin 5 and VEGF in retinal pigment epithelial cells: Involvement of NFAT5

Margrit Hollborn,[1] Stefanie Vogler,[2] Andreas Reichenbach,[2] Peter Wiedemann,[1] Andreas Bringmann,[1] Leon Kohen[1,3]

[1]Department of Ophthalmology and Eye Hospital, University of Leipzig, Leipzig, Germany; [2]Paul Flechsig Institute of Brain Research, University of Leipzig, Leipzig, Germany; [3]Helios Klinikum Aue, Aue, Germany

Purpose: High intake of dietary salt increases extracellular osmolarity, which results in hypertension, a risk factor of neovascular age-related macular degeneration. Neovascular retinal diseases are associated with edema. Various factors and channels, including vascular endothelial growth factor (VEGF) and aquaporins (AQPs), influence neovascularization and the development of edema. Therefore, we determined whether extracellular hyperosmolarity alters the expression of VEGF and AQPs in cultured human retinal pigment epithelial (RPE) cells.

Methods: Human RPE cells obtained within 48 h of donor death were prepared and cultured. Hyperosmolarity was induced by the addition of 100 mM NaCl or sucrose to the culture medium. Alterations in gene expression and protein secretion were determined with real-time RT–PCR and ELISA, respectively. The levels of signaling proteins and nuclear factor of activated T cell 5 (NFAT5) were determined by western blotting. DNA binding of NFAT5 was determined with EMSA. NFAT5 was knocked down with siRNA.

Results: Extracellular hyperosmolarity stimulated VEGF gene transcription and the secretion of VEGF protein. Hyperosmolarity also increased the gene expression of AQP5 and AQP8, induced the phosphorylation of p38 MAPK and ERK1/2, increased the expression of HIF-1α and NFAT5, and induced the DNA binding of NFAT5. The hyperosmotic expression of VEGF was dependent on the activation of p38 MAPK, ERK1/2, JNK, PI3K, HIF-1, and NFAT5. The hyperosmotic induction of AQP5 was in part dependent on the activation of p38 MAPK, ERK1/2, NF-κB, and NFAT5. Triamcinolone acetonide inhibited the hyperosmotic expression of VEGF but not AQP5. The expression of AQP5 was decreased by hypoosmolarity, serum, and hypoxia.

Conclusions: Hyperosmolarity induces the gene transcription of AQP5, AQP8, and VEGF, as well as the secretion of VEGF from RPE cells. The data suggest that high salt intake resulting in osmotic stress may aggravate neovascular retinal diseases and edema via the stimulation of VEGF production in RPE. The downregulation of AQP5 under hypoxic conditions may prevent the resolution of edema.

Systemic hypertension affects a large proportion of the adult population and has widespread effects on the sensory retina. High blood pressure may result in hypertensive retinopathy and is a major risk factor of diabetic retinopathy [1-3]. Control of blood pressure prevents vision loss from diabetic retinopathy, independently of glycemia [4,5]. Hypertension is also a risk factor of neovascular age-related macular degeneration (AMD) [6,7]; however, it has been shown that antihypertensive medications do not decrease the risk of AMD [8]. The molecular mechanisms of hypertensive effects on the retina are little understood. Hypertension-induced mechanical stress [9] may induce the expression of vascular endothelial growth factor (VEGF) in vascular endothelial and retinal pigment epithelial (RPE) cells [9,10]. Because VEGF is the most relevant factor that induces retinal angiogenesis and hyperpermeability of the blood–retinal barrier [11], increased production of VEGF will aggravate the development of retinal disorders associated with neovascularization and edema.

A major condition that causes systemic hypertension is the increase in extracellular osmolarity that results from an increased extracellular NaCl level following the high intake of dietary salt [12]. The blood pressure-raising effect of dietary salt increases with age, in particular due to increased vessel stiffness and age-related impairment of renal NaCl excretion [13]. High extracellular NaCl was shown to exacerbate experimental diabetic retinopathy [14]. High extracellular osmolarity has various effects on the retina, including a decrease in the standing potential of the eye [15] that originates from the RPE [16], alteration in the membrane potential of the RPE [17], decreases of electroretinogram waves [18], and the induction of neutrophil adhesion to vascular endothelia [19], an early event of tissue inflammation in diabetic retinopathy [20].

Correspondence to: Margrit Hollborn, Department of Ophthalmology and Eye Hospital, University of Leipzig, Faculty of Medicine, Liebigstrasse 10-14, D-04103 Leipzig, Germany; Phone : +49 (0) 341 97 21 561; FAX : +49(0) 341 97 21 659 ; email: hollbm@medizin.uni-leipzig.de

Osmotic conditions also regulate the tightness of the outer blood–retinal barrier constituted by the RPE. A hyperosmotic solution at the basal side of the RPE induces a breakdown of the barrier, while a hypoosmotic solution increases the barrier tightness [17, 21]. In humans, a mannitol infusion that increases extracellular osmolarity results in a reversible opening of the blood–retinal barrier [22]. The development of retinal edema is an important vision-threatening condition of ischemic and inflammatory retinal diseases, including diabetic retinopathy and neovascular AMD [23, 24]. Normally, glial and RPE cells clear excess fluid from the retinal tissue [25, 26] by transcellular transport of osmolytes and water; the water transport is facilitated by aquaporin (AQP) water channels [27, 28]. The fluid clearance capacity of glial and RPE cells can be exceeded when excess blood-derived fluid enters the retina and/or when the cells alter the expression of ion channels, transporters, and AQPs [29]. AQPs are a family of proteins that facilitate water transport across membranes in dependence on osmotic and hydrostatic gradients [30]. Human RPE cells were shown to express a variety of AQP subtypes [31].

Because systemic hypertension is a risk factor of neovascular AMD [6,7] and while antihypertensive medications do not alter the risk of the disease [8], we assume that further pathogenic conditions associated with hypertension, e.g., salt-induced extracellular hyperosmolarity, may influence the development of neovascularization and edema in the aged retina. To prove this assumption, we determined whether increased extracellular NaCl and osmolarity induce the expression of VEGF in cultured human RPE cells. We found that these conditions induce VEGF expression and secretion. In further experiments, we determined which intracellular signal transduction pathways and transcription factors mediate the effects of hyperosmolarity on the expression of VEGF. Because the resolution of osmotic gradients across membranes is facilitated by AQP water channels [30], we also determined whether high extracellular osmolarity alters the expression of AQPs in RPE cells. We found a high hyperosmotic induction of AQP5 and AQP8 in the cells. Because AQP8 mainly mediates mitochondrial ammonia transport [32, 33], while AQP5 plays an important role in transporting water across epithelia in other tissues [34-36], we further investigated the intracellular signal transduction pathways and transcription factors that mediate the effects of hyperosmolarity on the expression of AQP5, and determined additional factors and conditions that regulate the expression of AQP5. We found that the hyperosmotic expression of VEGF and AQP5 is, at least in part, induced by the activity of nuclear factor of activated T cell 5 (NFAT5), the classical transcription factor that regulates cellular responses to osmotic stress [37, 38]. The results may suggest that a high intake of dietary salt may aggravate neovascularization and edema by direct effects of high extracellular NaCl and osmolarity on RPE cells, independently of hypertension.

METHODS

Materials: Tissue culture components and solutions were purchased from Gibco BRL (Paisley, UK). Recombinant human VEGF-A_{165}, platelet-derived growth factor (PDGF)-BB, and tumor necrosis factor (TNF)-α were purchased from R&D Systems (Abingdon, UK). Interleukin (IL)-1β was purchased from Reliatech (Wolfenbüttel, Germany). AG490, activated coagulation factor X (FXa), the inhibitor of the hypoxia-inducible transcription factor 1 (HIF-1) 3-[2-(4-adamantan-1-yl-phenoxy)-acetylamino]-4-hydroxybenzoic acid methyl ester, LY294002, matrix metalloproteinase (MMP)-2 (active form), PD98059, rottlerin, SP600125, and SU1498 were purchased from Calbiochem (Bad Soden, Germany). AG1478 was purchased from Alexis (Grünberg, Germany), and Stattic was purchased from Enzo Life Science (Lörrach, Germany). Caffeic acid phenethyl ester and SB203580 were purchased from Tocris (Ellisville, MO). Human-specific small interfering RNA (siRNA) against NFAT5 (sc-43968) and nontargeted control siRNA-A (sc-37007) were obtained from Santa Cruz Biotechnology (Heidelberg, Germany). α-Thrombin and all other agents used were purchased from Sigma-Aldrich (Taufkirchen, Germany), unless stated otherwise.

The following antibodies were used: rabbit anti-human extracellular signal-regulated kinases 1 and 2 (ERK1/2, p44/p42; 19 ng/ml; Cell Signaling, Frankfurt/M., Germany), a rabbit anti-phosphorylated ERK1/2 (95 ng/ml; Cell Signaling), a rabbit anti-human p38 mitogen-activated protein kinase (p38 MAPK; 8 ng/ml; Cell Signaling), a rabbit anti-human phosphorylated p38 MAPK (27 ng/ml; Cell Signaling), a rabbit anti-human NFAT5 (1 µg/ml; Santa Cruz), a rabbit anti-human nuclear factor (NF)-κB p65 (144 ng/ml; Cell Signaling), a rabbit anti-human signal transducer and activator of transcription 3 (STAT3; 89 ng/ml; Cell Signaling), a rabbit anti-human histone H3 (160 ng/ml; Cell Signaling), a rabbit anti-GAPDH (12 ng/ml; Cell Signaling), an anti-rabbit IgG conjugated with alkaline phosphatase (35 ng/ml; Cell Signaling), a rabbit anti-AQP5 (2 µg/ml; Santa Cruz), a mouse anti-vimentin (V9; 1.5 µg/ml; DakoCytomation, Hamburg, Germany), a Cy2-coupled goat anti-mouse IgG (3.5 µg/ml; Jackson ImmunoResearch, Suffolk, UK), and a Cy3-coupled goat anti-rabbit IgG (3.7 µg/ml; Jackson).

Cell culture: The use of human material was approved by the Ethics Committee of the University of Leipzig, and

was performed according to the terms of the Declaration of Helsinki. Human RPE cells were obtained from post-mortem donors within 48 h of death, and were prepared and cultured as described [39]. Near-confluent cultures were growth arrested in medium without serum for 16 h; subsequently, serum-free media with and without test substances were added. Hyperosmotic media were made up by adding 100 mM NaCl or sucrose. The hypoosmotic medium (60% osmolarity) was made up by adding distilled water. Blocking agents were preincubated for 30–60 min.

Preparation of total RNA: Total RNA was extracted with the RNeasy Mini Kit (Qiagen, Hilden, Germany). The quality of the RNA was analyzed by agarose gel electrophoresis. The A_{260}–A_{280} ratio of the optical density was measured using the NanoDrop 1000 device (Peqlab, Erlangen, Germany), and was between 1.8 and 2.1 for all RNA samples, indicating sufficient quality. After treatment with DNase I (Roche, Mannheim, Germany), cDNA was synthesized from 1 µg of total RNA using the RevertAid H Minus First Strand cDNA Synthesis kit (Fermentas, St. Leon-Roth, Germany).

Real-time RT–PCR: Real-time RT–PCR was performed with the Single-Color Real-Time PCR Detection System (BioRad, Munich, Germany) using primer pairs described in Table 1. The PCR solution contained 1 µl of cDNA, a specific primer set (0.2 µM each), and 10 µl of a 2× mastermix (iQ SYBR Green Supermix, BioRad) in a final volume of 20 µl. The following conditions were used: initial denaturation and enzyme activation (one cycle at 95 °C for 3 min); denaturation, amplification, and quantification (45 cycles at 95 °C for 30 s, 58 °C for 20 s, and 72 °C for 45 s); and a melting curve (55 °C, with the temperature gradually increased 0.5 °C up to 95 °C). The amplified samples were analyzed by standard agarose gel electrophoresis. mRNA expression was normalized to the level of β-actin mRNA. Changes in mRNA expression were calculated according to the $2^{-\Delta\Delta CT}$ method (CT, cycle threshold), with $\Delta CT=CT_{\text{target gene}} - CT_{\text{actb}}$ and $\Delta\Delta CT=\Delta CT_{\text{treatment}} - \Delta CT_{\text{control}}$.

mRNA stability: Cells were first treated with NaCl (+ 100 mM) or double-distilled water for 12 h, followed by the addition of actinomycin D (5 µg/ml). Total RNA was isolated at 1.5, 3, 4.5, and 6 h after the addition of actinomycin D, and mRNA expression was determined by real-time RT–PCR analysis. The vehicle control (1:500 ethanol) had no effect on AQP5 and VEGF mRNA stability (not shown).

ELISA: Cells were stimulated with iso- and hyperosmotic (+ 100 mM NaCl) media without serum in the absence and presence of blocking substances. The supernatants were collected after 6 and 24 h, and the level of VEGF-A_{165} in the cultured media (200 µl) was determined by ELISA (R&D Systems).

Western blot analysis of cellular proteins: The cells were seeded at 5×10^5 cells per well in six-well plates in 1.5 ml complete medium, and were allowed to grow up to a confluency of ~80%. After growth arrest for 16 h, the cells were treated with test substances and a hyperosmotic medium (+ 100 mM NaCl) for 20 min, 6 h, and 24 h, respectively. Then, the medium was removed, the cells were washed twice with pre-chilled phosphate-buffered saline (pH 7.4; Invitrogen, Paisley, UK), and the monolayer was scraped into 150 µl of lysis buffer (Mammalian Cell Lysis-1 Kit; Sigma). The total cell lysates were centrifuged at 10,000 × *g* for 10 min, and the supernatants were analyzed by immunoblotting. Equal amounts of protein (for the detection of intracellular signal transduction proteins and GAPDH: 30 µg; of NFAT5: 70 µg) were separated by 10% SDS–PAGE. Immunoblots were probed with primary and secondary antibodies, and immunoreactive bands were visualized using 5-bromo-4-chloro-3-indolyl phosphate/nitro blue tetrazolium.

Nuclear protein extraction and western blot analysis of nuclear proteins: The cells (~90% of confluency) were growth arrested for 5 h and then treated with a hyperosmotic medium (+ 100 mM NaCl) for 24 h. Thereafter, the medium was removed; the cells were washed with ice-cold phosphate-buffered saline and harvested using StemProAccutase (Gibco). Nuclear extracts were prepared by cell lysis in ice-cold buffer A (10 mM HEPES, pH 7.9; 1.5 mM $MgCl_2$; 10 mM KCl; 1 mM dithiothreitol; 0.5 mM phenylmethylsulfonyl fluoride; 1 µM Na_3VO_4; 0.4% NP-40) for 20 min on ice with vortexing. After centrifugation at 13,000 × *g* for 20 s, nuclear pellets were resuspended in buffer B (20 mM HEPES, pH 7.9; 420 mM NaCl; 1.5 mM $MgCl_2$; 0.2 mM EDTA; 0.2 mM phenylmethylsulfonyl fluoride; 1 µM Na_3VO_4). Cell nuclei were lysed by intensive shaking using a vortexer at 4 °C for 30 min. Lysates were cleared by centrifugation at 13,000 × *g* for 2 min. Equal amounts of protein (20 µg) were separated by 10% SDS–PAGE; immunoreactive bands were visualized using 5-bromo-4-chloro-3-indolyl phosphate/nitro blue tetrazolium.

Electrophoretic mobility shift assay (EMSA): EMSA was performed with the DIG Gel Shift Kit 2nd Generation (Roche) according to the manufacturer's instructions, using the following oligonucleotides, which contained binding sites for NFAT5 (cursive letters): GTGAAGCACCAAA*TGGAAAATCACC*GGCATGGAGT and GTGACTCCATGC*CGGTGATTTTCCA*TTTGGTGCTT. Gel shift reaction was performed with 4 µg of nuclear extract in a total volume of 20 µl for 25 min at room temperature. To check the specificity of DNA–protein interaction, unlabeled double-stranded oligonucleotides were used as competitors in 200-fold excess.

Electrophoresis was performed with a 4% non-denaturing PAGE; the separated oligonucleotide-protein complexes were transferred to a positively charged nylon membrane by electroblotting. DIG-labeled DNA fragments were detected with an anti-DIG antibody, and immunoreactive bands were visualized using 5-bromo-4-chloro-3-indolyl phosphate/nitro blue tetrazolium.

siRNA transfection: Cells were seeded at 7×10^4 cells per well in 12-well culture plates and were allowed to grow up to a confluency of 60%–80%. Thereafter, the cells were transfected with NFAT5 siRNA and nontargeted siRNA (each 5 nM), respectively, using a HiPerfect reagent (Qiagen, Hilden, Germany) in F-10 medium containing 10% fetal bovine serum (Invitrogen) according to the manufacturer's

Table 1. Primer pairs used in PCR experiments. S, sense. AS, anti-sense.

Gene and Accession	Primer sequence (5′→3′)	Amplicon (bp)
ACTB	F: ATGGCCACGGCTGCTTCCAGC	237
NM_001101	R: CATGGTGGTGCCGCCAGACAG	
VEGFA	F: CCTGGTGGACATCTTCCAGGAGTA	407; 347; 275
NM_001025370	R: CTCACCGCCTCGGCTTGTCACA	
NFAT5	F: TCACCATCATCTTCCCACCT	174
XM_005255777.1	R: CTGCAATAGTGCATCGCTGT	
HIF1α	F: CACAGAAATGGCCTTGTGAA	214
NM_001530.3	R: CCAAGCAGGTCATAGGTGGT	
AQP0	F: TGTACTGGGTAGGCCCAATC	237
NM_012064	R: CCCCTCCACGTAAACTCAGA	
AQP1	F: GTCCAGGACAACGTGAAGGT	218
NM_198098.1	R: GAGGAGGTGATGCCTGAGAG	
AQP2	F: CCTCTATTGCCCAGATTGGA	223
NM_000486.5	R: GGGGAAGCTTTGGAAATAGC	
AQP3	F: AGACAGCCCCTTCAGGATTT	226
NM_004925.3	R: TCCCTTGCCCTGAATATCTG	
AQP4	F: GGAATTTCTGGCCATGCTTA	226
NM_001650.4	R: AGACTTGGCGATGCTGATCT	
AQP5	F: ACTGGGTTTTCTGGGTAGGG	184
NM_001651.2	R: GTGGTCAGCTCCATGGTCTT	
AQP6	F: CACTCAAAGGGAGCCAGAAG	162
NM_001652	R: CGCACTCACAGAATGCAGAT	
AQP7	F: GTGATAGGCATCCTCGTGGT	186
NM_001170.1	R: ATAGGCACCCAGAAGTGGTG	
AQP8	F: TCCTGAGGAGAGGTTCTGGA	157
NM_001169.2	R: AGGGCCCTTTGTCTTCTCAT	
AQP9	F: AGCCACCTCTGGTCTTGCT	167
NM_020980.3	R: ATGTAGAGCATCCCCTGGTG	
AQP10	F: GCCTGGGAACAACAGTCATT	155
NM_080429.2	R: TGAGAAGCCTGAGTCCTGGT	
AQP11	F: GGCTGGCTCCTTCTTTAGGT	181
NM_173039.1	R: CCGGTGTTTTCCATATGAGG	
AQP12	F: CTTCTTCTTTGCCACCTTCG	240
NM_198998.1	R: AACTCCTGCAGGGACACAGT	

instructions. After 48 h, the medium was removed and fresh iso- or hyperosmotic medium without serum was added for 2, 6, and 24 h, respectively. Total RNA was extracted, and NFAT5, AQP5, and VEGF mRNA levels were determined with real-time RT–PCR analysis. The VEGF content of the cultured media was determined with ELISA.

Immunocytochemistry: Cultured cells were fixed in 0.4% paraformaldehyde for 15 min. After several washing steps in buffered saline, the cells were incubated in 5% normal goat serum, 0.3% Triton X-100, and 1% DMSO (DMSO) in saline for 1 h at room temperature and, subsequently, in a mixture of primary antibodies overnight at 4 °C. After washing in saline plus 0.3% Triton X-100 and 1% DMSO, secondary antibodies and Hoechst 33,258 (1:500) were applied for 1 h at room temperature. Images were taken with a confocal laser scanning microscope (LSM 510 Meta; Zeiss, Oberkochen, Germany).

Statistics: For each test, at least three independent experiments using cells from different donors were performed in triplicate. The numbers of independent experiments (n) hold for both stimulated and control conditions. Data are expressed as means ± SEM. Statistical analysis was made using Prism (Graphpad Software, San Diego, CA). Significance was determined by one-way ANOVA followed by Bonferroni's multiple comparison test and Mann–Whitney *U* test, and was accepted at $p<0.05$.

RESULTS

Osmolarity-dependent expression of VEGF: To determine whether high extracellular NaCl and/or osmolarity alter the expression of VEGF, we stimulated cultured human RPE cells with media that were made hyperosmotic by the addition of 100 mM NaCl or sucrose. As shown in Figure 1A,B, high NaCl induced time-dependent increases in the VEGF mRNA level and secretion of VEGF protein from the cells. Increases in VEGF expression and secretion were also observed after the addition of 100 mM sucrose to the medium (Figure 1C,D). The effect of high extracellular NaCl on the cellular VEGF mRNA level was dose-dependent (Figure 1E). Culturing the cells in a hypoosmotic medium (60% osmolarity) decreased the cellular VEGF mRNA level after 24 h of stimulation (Figure 1F) but did not alter the secretion of VEGF (n=5; not shown). Anti-inflammatory steroids such as triamcinolone acetonide are clinically used for the rapid resolution of retinal edema [40]. Triamcinolone acetonide is known to inhibit the hypoxic secretion of VEGF from RPE cells [41]. Triamcinolone also fully prevented the hyperosmotic increases in VEGF mRNA (Figure 1A) and secretion of VEGF (Figure 1B).

Regulation of the hyperosmotic induction of VEGF: The hyperosmotic increase in VEGF gene expression resulted from the stimulation of gene transcription (Figure 2A) and not from altered mRNA stability (Figure 2B). The hyperosmotic increase in VEGF gene transcription was nearly fully abrogated by inhibitors of p38 MAPK, ERK1/2, c-Jun NH_2-terminal kinase (JNK), and phosphatidylinositol-3 kinase (PI3K)-Akt signal transduction pathways (Figure 3A). The inhibitors also decreased the hyperosmotic secretion of VEGF (Figure 3B). Selective antagonists of PDGF and epidermal growth factor (EGF) receptor tyrosine kinases, AG1296 and AG1478, did not inhibit the hyperosmotic expression of VEGF (Figure 3A), suggesting that the upregulation of VEGF was not mediated by autocrine/paracrine PDGF and EGF signaling. In agreement with a recent study [42], we found that hyperosmotic stimulation for 20 min induced increased phosphorylation of p38 MAPK protein (Figure 3C). In addition, hyperosmotic stimulation induced the phosphorylation of ERK1/2 proteins (Figure 3C). The phosphorylation of p38 and ERK1/2 was not stimulated by chemical hypoxia for 20 min (Figure 3C).

Expression of AQP genes: The resolution of osmotic gradients across membranes is facilitated by AQP water channels [30]. We compared the expression levels of AQP genes in RPE cells, which were freshly isolated from human post-mortem donor eyes, and in cultured human RPE cells. In agreement with a previous study [31], we found that both freshly isolated and cultured RPE cells did not contain AQP2 gene transcripts (Figure 4A). Transcripts of AQP4, 6, 7, 10, and 12 genes were detectable in freshly isolated cells, but not in cultured cells (Figure 4A). The expression levels of AQP1, 5, 8, 9, and 11 genes were smaller in cultured cells than in freshly isolated cells, as indicated by the significantly ($p<0.05$) increased ΔCT values (Figure 4A). The expression levels of AQP0 and AQP3 genes were not different between freshly isolated and cultured cells (Figure 4A). The data indicate that human RPE cells in situ contain gene transcripts of various AQP subtypes, and that the expression of various AQP genes is downregulated in cultured cells compared to freshly isolated cells. It was shown that cultured human RPE cells display immunoreactivities for AQP1, 3, and 9 proteins [31, 43]. We found that the cells also display AQP5 immunoreactivity (Figure 4B).

Transcriptional regulation of AQP5: The stimulation of cultured RPE cells with a hyperosmotic medium (+ 100 mM NaCl) induced strong time-dependent increases in AQP5 and AQP8 mRNA levels, while the gene expression of further AQPs investigated was not or only moderately altered (Figure 5A). An increase in the AQP5 mRNA level was also observed after the addition of 100 mM sucrose to the medium (Figure

5B). The effect of high extracellular NaCl on the cellular AQP5 mRNA level was dose-dependent (Figure 5C). Extracellular hypoosmolarity decreased the level of AQP5 mRNA (Figure 5D). The AQP5 mRNA level remained largely unaltered in response to oxidative stress induced by the addition of H_2O_2 (20 µM; n=7; not shown) and in the presence of high (25 mM) glucose (Figure 5E), VEGF (10 ng/ml; n=8), PDGF (10 ng/ml; n=6), IL-1β (10 ng/ml; n=6), TNFα (10 ng/ml; n=5), MMP-2 (10 ng/ml; n=3), arachidonic acid (5 µM; n=4), prostaglandin E_2 (10 ng/ml; n=8), thrombin (10 U/ml; n=7), and coagulation factor Xa (1 U/ml; n=6), respectively (data not shown). The AQP5 mRNA level was decreased in the presence of the hypoxia mimetic $CoCl_2$ [44], and strongly reduced in the presence of fetal bovine serum (Figure 5E). The data suggest that the gene expression of AQP5 in RPE cells is relatively specifically regulated by osmotic gradients, hypoxia, and blood serum. Triamcinolone acetonide decreased the AQP5 mRNA level under isoosmotic conditions, but did not prevent the hyperosmotic induction of AQP5 gene expression (Figure 5F).

Regulation of the hyperosmotic induction of AQP5: Hyperosmotic AQP5 expression was induced by the stimulation of gene transcription (Figure 6A) and not by altered mRNA stability (Figure 6B). The hyperosmotic expression of AQP5

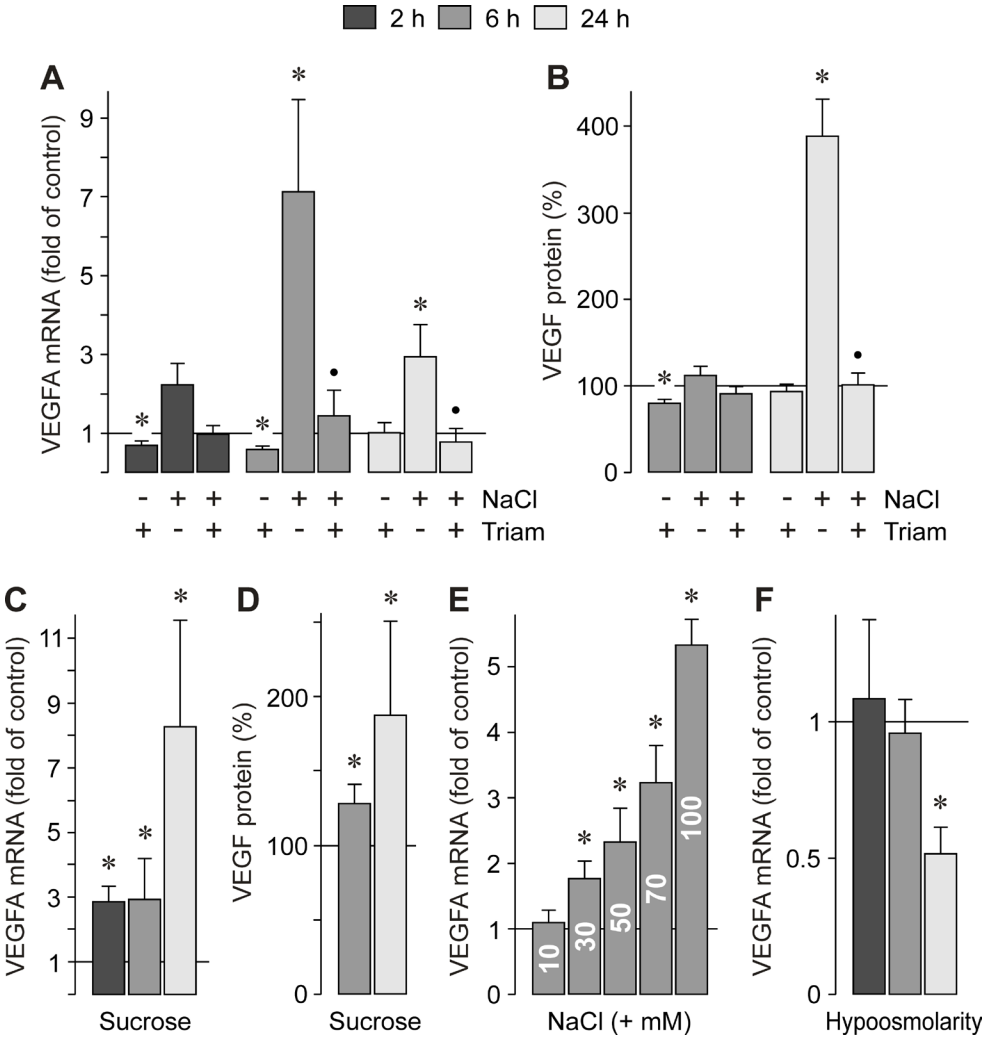

Figure 1. Osmolarity-dependent production of VEGF in RPE cells. The mRNA expression (**A, C, E, F**) was determined with real-time RT–PCR analysis and is expressed as a fold of isoosmotic unstimulated control. The level of VEGF-A_{165} protein in the cultured media (**B, D**) was determined with ELISA and is expressed as a percentage of isoosmotic unstimulated control (100%, corresponding to 169.1±38.9 [**B**, 6 h], 230.6±55.1 [**B**, 24 h], and 525.0±90.6 pg/ml VEGF[**D**], respectively). **A.** Relative expression level of *VEGFA* in cells cultured for 2, 6, and 24 h in isoosmotic (- NaCl) and hyperosmotic (+ 100 mM NaCl) media in the absence (- Triam) and presence (+ Triam) of triamcinolone acetonide (50 µM). **B.** Release of VEGF protein from RPE cells measured under hyperosmotic conditions. The cells were stimulated for 6 and 24 h, respectively, with hyperosmotic medium (+ 100 mM NaCl) in the absence (- Triam) and presence (+ Triam) of triamcinolone acetonide (50 µM). The data are expressed as a percentage of isoosmotic untreated control (100%). **C.** Effect of hyperosmotic medium (+ 100 mM sucrose) on the expression of *VEGFA*. **D.** Effect of hyperosmotic medium (+ 100 mM sucrose) on the release of VEGF protein from RPE cells. **E.** Dose-dependent effect of high extracellular NaCl on the cellular level of VEGF mRNA. The cells were cultured for 6 h in media that were made hyperosmotic by the addition of 10 to 100 mM NaCl. **F.** Effect of hypoosmotic medium (60% osmolarity) on the expression of *VEGFA*. Data are means ± SEM of n=4 (**C, D, E**), 5 (**F**), 7 (**B**), and 10 (**A**) independent experiments performed in triplicate. Significant difference versus isoosmotic unstimulated control: *p<0.05. Significant difference versus NaCl control: ●p<0.05.

was significantly ($p<0.05$) decreased by the inhibitors of p38 MAPK and ERK1/2 signal transduction pathways (Figure 7). Inhibitors of the PI3K signal transduction pathway and JNK activation had no effects (Figure 7). Furthermore, antagonists of PDGF and EGF receptor tyrosine kinases, and of the VEGF receptor-2, did not inhibit the hyperosmotic upregulation of AQP5 (Figure 7). The data suggest that hyperosmotic AQP5 gene expression is in part dependent on the activation of p38 MAPK and ERK1/2 signal transduction pathways.

Role of transcription factors in the hyperosmotic induction of AQP5 and VEGF: The VEGF gene expression induced by chemical hypoxia and hyperosmolarity were not additive (Figure 8A). This suggests the involvement of (at least in part) common mechanisms of the transcriptional activation of VEGF under both conditions. HIF-1 and STAT3 are known transcriptional activators of VEGF [45, 46]. In RPE cells, hyperosmotic challenges increased the gene expression of HIF-1α while hypoosmolarity had no effect (Figure 8B). To reveal whether HIF-1 activity is required for the hyperosmotic induction of AQP5 and VEGF in RPE cells, we tested an HIF inhibitor [47]. The HIF inhibitor decreased the hyperosmotic induction of VEGF by approximately 50% (Figure 8C) and almost completely abrogated the hyperosmotic secretion of VEGF protein (Figure 8D). On the other hand, the Janus kinase (JAK)-2 inhibitor AG490 [48], which inhibits the DNA binding of STAT3; the STAT3 inhibitor Stattic [49]; and the inhibitor of the nuclear transcription factor NF-κB, caffeic acid phenethyl ester [50] had no significant effects on the hyperosmotic induction of VEGF gene transcription (Figure 8C) and the hyperosmotic secretion of VEGF (Figure 8D). The data suggest that the hyperosmotic production of VEGF is in part mediated by HIF-1 but not by STAT3 or NF-κB. In contrast, hyperosmotic AQP5 gene expression was significantly ($p<0.05$) decreased by the NF-κB inhibitor, while the HIF inhibitor, the JAK2 inhibitor, and the STAT3 inhibitor were without effects (Figure 8E).

In various cell systems, the transcriptional activity of NFAT5 is critical for cell survival under hyperosmotic conditions [37, 38]. We found that hyperosmotic media transiently increased the gene expression of NFAT5 in RPE cells while a hypoosmotic medium decreased the expression of NFAT5 (Figure 9A). The effect of high extracellular NaCl on the cellular NFAT5 mRNA level was dose-dependent (Figure 9B). Hyperosmolarity also increased the cellular (Figure 9C) and nuclear levels (Figure 9D, E) of the NFAT5 protein, while hypoosmolarity decreased the cellular level of NFAT5 protein (Figure 9C). In addition, hyperosmolarity increased the nuclear level of p65/NF-κB protein, while the nuclear level of STAT3 protein remained unchanged (Figure 9E). EMSA showed that hyperosmolarity induced the DNA binding of

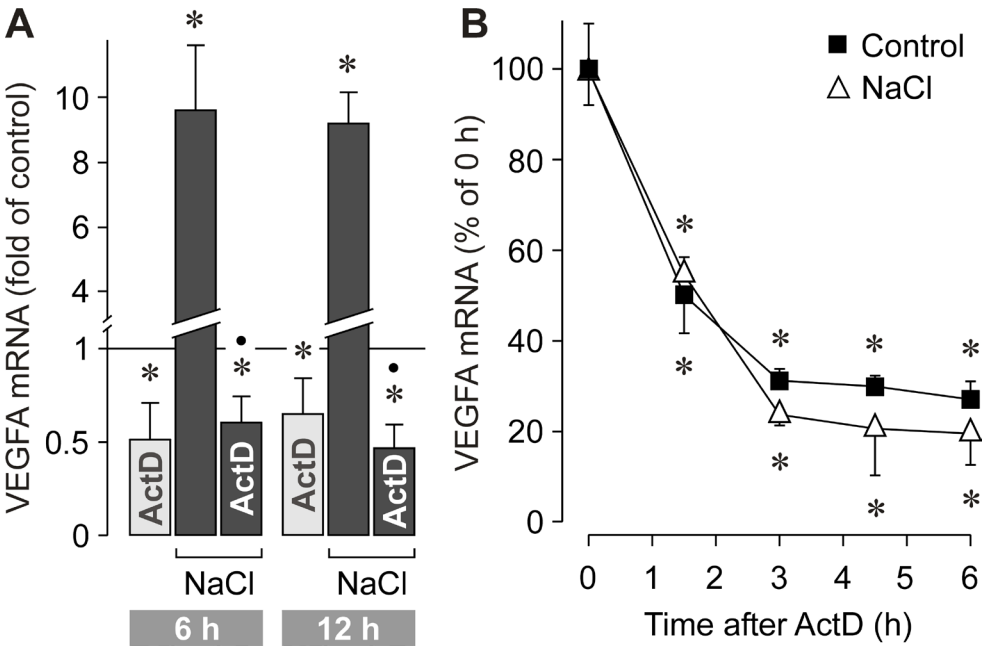

Figure 2. The hyperosmotic upregulation of VEGF is induced by the stimulation of gene transcription. mRNA expression was measured with real-time RT–PCR analysis. **A.** Inhibition of the gene transcription by actinomycin D (ActD; 5 µg/ml) abrogated the increase in VEGF mRNA induced by hyperosmotic (+ 100 mM NaCl) medium. The data were obtained after 6 (n=4) and 12 h (n=5) of stimulation, respectively, and are expressed as folds of isoosmotic unstimulated control. Actinomycin D was preincubated for 30 min. **B.** The stability of VEGF mRNA did not differ between isoosmotic (control; n=6) and hyperosmotic (+ 100 mM NaCl; n=4) conditions. The cells were first treated with isoosmotic (control) and hyperosmotic (+ 100 mM NaCl) media for 12 h, followed by the addition of actinomycin D (5 µg/ml). Total RNA was isolated at different time periods after the addition of actinomycin D. Data are means ± SEM obtained in independent experiments performed in triplicate, and expressed in percent of 0-h control. Significant differences versus isoosmotic unstimulated control (**A**) and 0 h (**B**): *$p<0.05$. Significant difference versus NaCl control: ●$p<0.05$.

the NFAT5 protein (Figure 9F). Chemical hypoxia did not induce increased levels of NFAT5 mRNA (Figure 9A) and protein (Figure 9C). Similarly, hypoxic conditions induced by culturing the cells in 1% O_2 did not alter the gene expression of NFAT5 (Figure 9A). In addition, oxidative stress induced by the addition of H_2O_2 (20 µM) did not increase the nuclear level of the NFAT5 protein (n=3; not shown). The data suggest that the expression of NFAT5 in RPE cells is regulated by osmotic changes, but not by hypoxia and oxidative stress.

To determine whether the hyperosmotic expression of AQP5 and VEGF depends on the transcriptional activity of NFAT5, we tested the NFAT5 inhibitor rottlerin [51]. Rottlerin inhibited the hyperosmotic gene expression of AQP5 (Figure 10A) and VEGF (Figure 10B), as well as the hyperosmotic secretion of VEGF (Figure 10C). To confirm the involvement of NFAT5 activity in the hyperosmotic induction of AQP5 and VEGF with another method, we used siRNA to knock down NFAT5. The inhibitory activity of the siRNA was confirmed in cells cultured under isoosmotic (Figure 10D) and hyperosmotic conditions (Figure 10E). RPE cells transfected with NFAT5 siRNA displayed a significantly ($p<0.05$) reduced upregulation of AQP5 (Figure 10F) and VEGF expression (Figure 10G), and a significantly ($p<0.05$) reduced secretion of VEGF (Figure 10H) under hyperosmotic conditions compared to non-transfected cells. Transfection of the cells with nontargeted negative control siRNA had no significant effects on the hyperosmotic induction of AQP5 and VEGF gene expression (Figure 10F,G), or on the hyperosmotic secretion of VEGF from RPE cells (Figure 10H).

DISCUSSION

Systemic hypertension increases the risk of neovascular AMD [6, 7]. One main factor that causes hypertension is high salt intake resulting in increased extracellular osmolarity [12]. Because antihypertensive medications do not decrease the risk of AMD [8], we assume that further pathogenic conditions associated with hypertension, e.g., increased extracellular NaCl level and/or increased extracellular osmolarity,

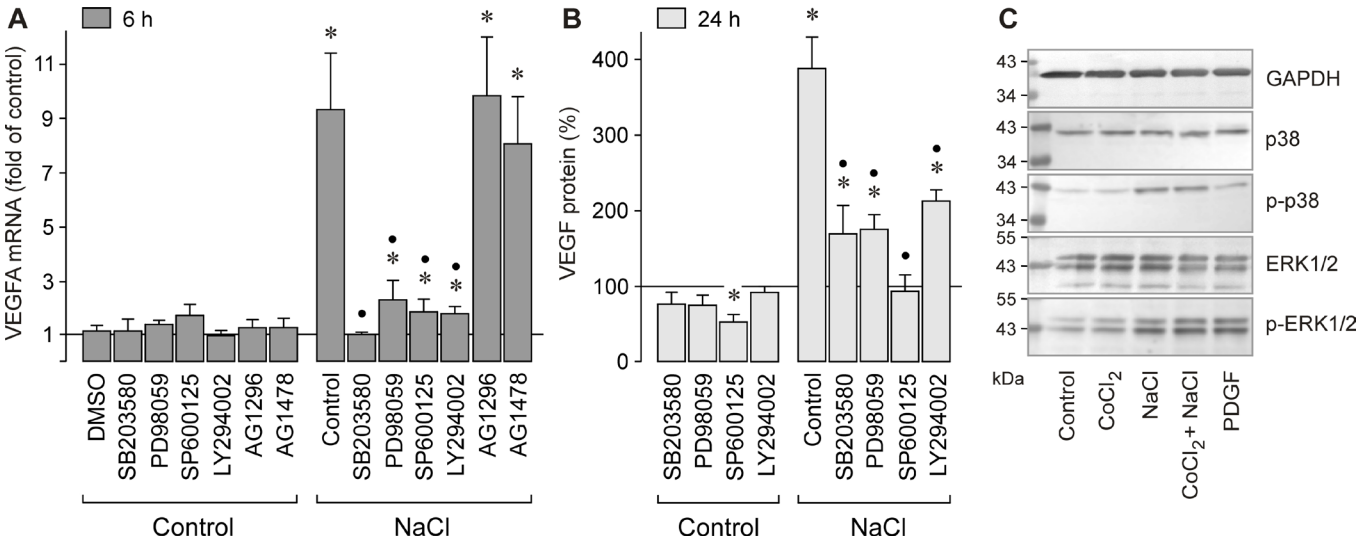

Figure 3. Involvement of signal transduction pathways in the hyperosmotic induction of VEGF in RPE cells. The mRNA level (**A**) was determined with real-time RT–PCR analysis in cells cultured 6 h under iso- (control) and hyperosmotic conditions (+ 100 mM NaCl), and is expressed as folds of isoosmotic unstimulated control. The level of VEGF-A_{165} protein (**B**) was determined with ELISA in the media of cells cultured 24 h under iso- and hyperosmotic conditions, and is expressed in a percentage of isoosmotic unstimulated control (100%, corresponding to 281.7±45.8 pg/ml VEGF). The cytosolic protein levels (**C**) were determined by western blot analysis. **A.** The hyperosmotic upregulation of *VEGFA* was decreased by the inhibitor of p38 MAPK activation, SB203580 (10 µM; n=6); the inhibitor of ERK1/2 activation, PD98059 (20 µM; n=6); the JNK inhibitor SP600125 (10 µM; n=5); and the inhibitor of PI3K-related kinases, LY294002 (5 µM; n=6), respectively. The inhibitor of the PDGF receptor tyrosine kinase, tyrphostin AG1296 (10 µM; n=5), and the inhibitor of the EGF receptor tyrosine kinase, AG1478 (600 nM; n=5), did not inhibit the hyperosmotic upregulation of *VEGFA*. The vehicle control was made with DMSO (1%; n=3). **B.** The inhibitors of p38 MAPK (n=5), ERK1/2 (n=5), JNK (n=5), and PI3K (n=5) also decreased the secretion of VEGF induced by hyperosmotic stimulation. **C.** Stimulation of the cells for 20 min with $CoCl_2$ (150 µM) or hyperosmotic medium (+ 100 mM NaCl) induced the phosphorylation of p38 and ERK1/2 proteins. PDGF (10 ng/ml) was used as a positive control. Amounts of total proteins are shown above; amounts of phosphorylated proteins are shown below. Similar results were obtained in three independent experiments using cells from different donors. Bars represent means ± SEM obtained in independent experiments performed in triplicate. Significant difference versus isoosmotic unstimulated control: *$p<0.05$. Significant difference versus NaCl control: ●$p<0.05$.

may induce cellular alterations that favor angiogenesis and edema in the aged retina. Mechanical stretching and hypertension are known to stimulate the expression of VEGF in vascular endothelial and RPE cells [9, 10]. However, it is not known whether increased extracellular NaCl and/or increased osmolarity affect the expression of VEGF in retinal cells. We describe that hyperosmolarity induces transcriptional activation of the VEGF gene and secretion of VEGF protein from RPE cells (Figure 1A-D). The high NaCl- and sucrose-induced VEGF gene expression showed different time dependencies (Figure 1A,C), suggesting that both hyperosmolarity and alteration of the transmembrane NaCl gradient induce VEGF gene transcription. Because a decrease in the extracellular osmolarity results in a decreased expression of the VEGF gene (Figure 1F), transcriptional activation of the VEGF gene is directly related to the extracellular osmolarity.

Water transport through AQPs is crucially implicated in the resolution of osmotic gradients across membranes [30]. In agreement with a previous study [31], we found that both freshly isolated and cultured human RPE cells contain gene transcripts of various AQP subtypes. By using real-time RT–PCR, we compared the cellular levels of AQP gene transcripts in freshly isolated and cultured RPE cells, and found that the expression of various AQP genes is downregulated in cultured cells compared to freshly isolated cells (Figure 4A). The expression of AQP subtypes in human RPE cells is still

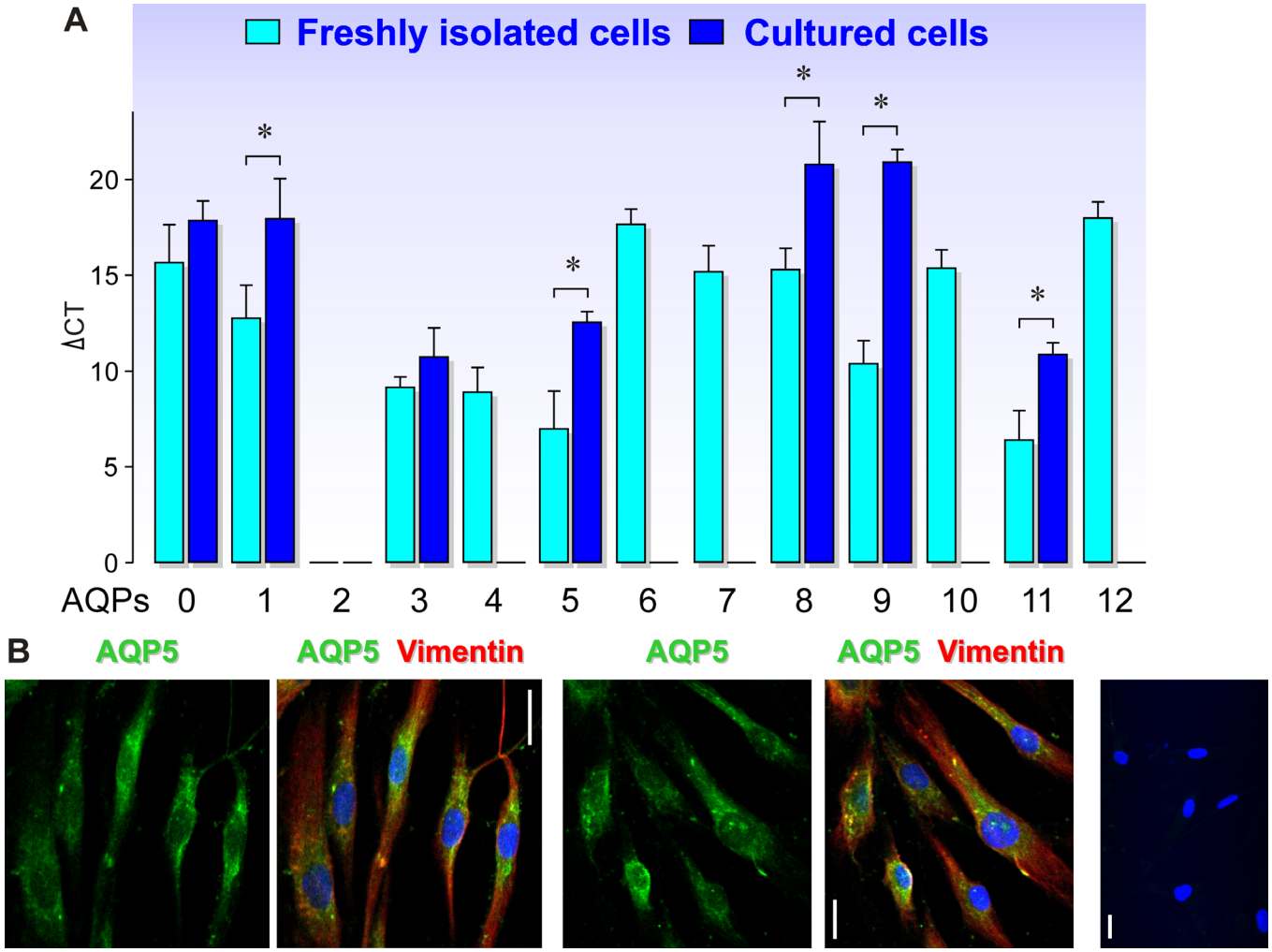

Figure 4. Expression of AQP subtypes in freshly isolated and cultured human RPE cells. **A.** Comparison of the expression levels of AQP1–12 genes in freshly isolated and cultured RPE cells. Bars represent means ± SEM normalized cycle thresholds (ΔCT) required to detect mRNA in real-time RT–PCR. The smaller the ΔCT value, the higher the cellular mRNA level. The values were obtained in four independent preparations of freshly isolated cells from different donors and in three independent cultures using cells from different donors, respectively. Significant difference: *p<0.05. **B.** Immunolabeling of cultured human RPE cells with antibodies against AQP5 (*green*) and vimentin (*red*). Cell nuclei were labeled with Hoechst 33,258 (*blue*). *Right:* Negative control cells stained without primary antibodies. Bars, 20 µm.

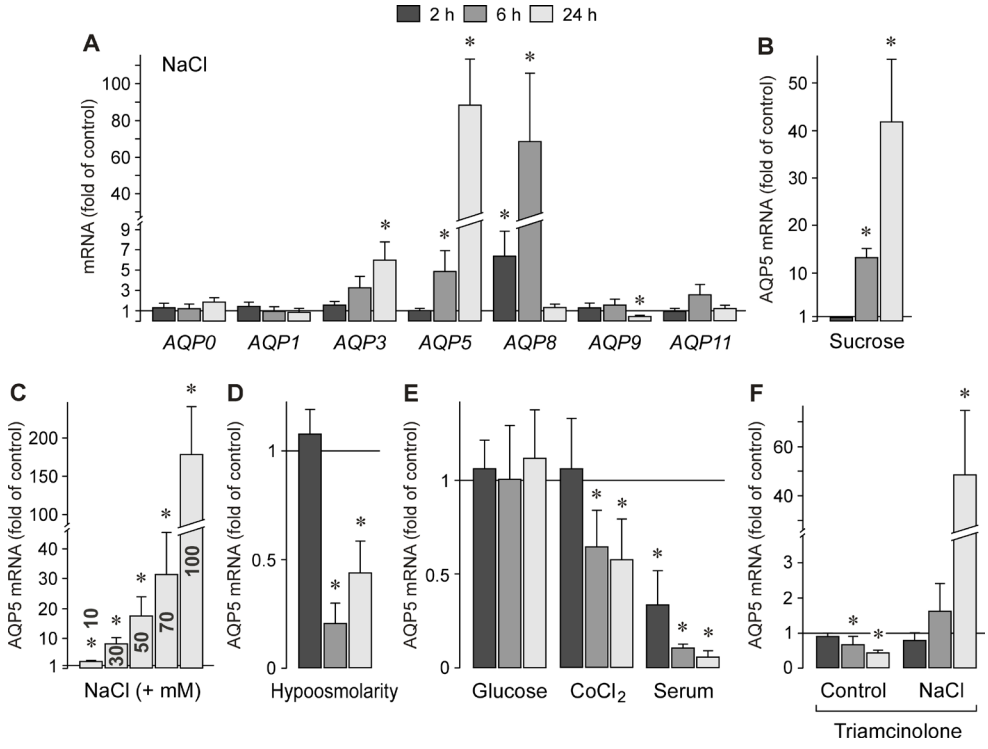

Figure 5. Regulation of the AQP5 gene expression in RPE cells. The mRNA levels were determined with real-time RT–PCR analysis after stimulation of the cells for 2, 6, and 24 h, and are expressed as folds of isoosmotic unstimulated control. **A.** Effect of hyperosmotic culture medium (+ 100 mM NaCl) on the gene expression level of various AQP subtypes (n=8). **B.** Effect of hyperosmotic medium (+ 100 mM sucrose) on the gene expression of AQP5 (n=4). **C.** Dose-dependent effect of high extracellular NaCl on the cellular level of AQP5 mRNA (n=4). The cells were cultured for 6 h in media that were made hyperosmotic by the addition of 10 to 100 mM NaCl. **D.** Effect of hypoosmotic medium (60% of control osmolarity) on the gene expression of AQP5 (n=6). **E.** Effects of high (25 mM) glucose (n=7), $CoCl_2$ (150 µM; n=8), and fetal bovine serum (10%; n=4) on the gene expression of AQP5. **F.** Regulation of AQP5 expression by triamcinolone acetonide (50 µM) under isoosmotic (control; n=8) and hyperosmotic (+ 100 mM NaCl; n=6) conditions. Data are means ± SEM obtained in independent experiments performed in triplicate. Significant difference versus isoosmotic unstimulated control: *p<0.05.

a matter of debate. A recent study described an absence of AQP6, 8, 10, and 12 gene transcripts in the human retina and sclera [52]. The reasons for the different results are unclear and might be related to different tissue and RNA preparation procedures, or to different PCR conditions.

We show that increased extracellular osmolarity highly induces the expression of AQP5 and AQP8 in RPE cells (Figure 5A). It is known that AQP8 mainly mediates mitochondrial ammonia transport [32, 33], while AQP5 mediates transepithelial water transport [34-36]. Therefore, we focused the following experiments on the regulation of the AQP5 expression in RPE cells. Because the high NaCl- and sucrose-induced upregulation of AQP5 displayed similar time dependencies (Figure 5A,B), we assume that hyperosmolarity, but not the alteration in the transmembrane NaCl gradient, induces AQP5 gene transcription. AQP5 gene expression was decreased by extracellular hypoosmolarity (Figure 5D) and the presence of blood serum and the hypoxia mimetic $CoCl_2$ (Figure 5E), respectively. The $CoCl_2$-induced decrease in AQP5 expression is in agreement with previous studies, which showed that hypoxia induces downregulation of AQP5 in lung epithelial cells [53], and that experimental retinal ischemia results in decreased retinal AQP5 gene expression [31].

In the following experiments, we determined the regulation of the hyperosmotic induction of VEGF and AQP5 in RPE cells. We found that the hyperosmotic induction of VEGF in RPE cells depends on the activation of p38 MAPK, ERK1/2, JNK, and PI3K signal transduction pathways (Figure 3A,B), and (at least in part) on HIF-1 activity (Figure 8C,D). Because blockades of each of these pathways alone decreased to a great degree the hyperosmotic expression of VEGF (Figure 3A), we assume that functional relations exist between the various intracellular signal transduction pathways. The results are in agreement with previous studies, which showed in various cell systems that the expression of VEGF is regulated by a positive signaling between HIF-1, ERK1/2, and PI3K-Akt [54,55], and that hyperosmolarity may induce VEGF expression via the induction of HIF-1α [56]. The lack of significant effects of an NF-κB inhibitor on the hyperosmotic VEGF expression (Figure 8C,D) is in agreement with a previous study that indicates that the human VEGF promoter does not contain a NF-κB DNA-binding consensus sequence [57]. Although STAT3 is a known

activator of VEGF expression [46], we found that STAT3 activity is not involved in the hyperosmotic induction of VEGF in RPE cells (Figure 8C,D). This fact is in agreement with the observation that hyperosmolarity did not increase the level of the nuclear STAT3 protein (Figure 9E).

The hyperosmotic expression of AQP5 was dependent in part on the activation of p38 MAPK and ERK1/2 signaling pathways, and on the transcriptional activity of NF-κB, but was independent of the activation of JNK, PI3K, JAK/STAT, and HIF-1 (Figure 7 and Figure 8E). Because blockers of p38 MAPK and ERK1/2 activation did not fully inhibit hyperosmotic AQP5 expression (Figure 7), further signaling molecules are likely involved. The present finding that the hyperosmotic expression of AQP5 in RPE cells was reduced by a NF-κB inhibitor (Figure 8E) is in contradiction with data obtained in various cell systems, which suggest that the activation of NF-κB induces the downregulation of AQP5 [58,59]. The reason for the conflicting results is unclear. However, because the transcription of the AQP5 gene slowly increased under hyperosmotic conditions and peaked after 24 h (Figure 5A,B), it is likely that the hyperosmotic AQP5 expression is indirectly induced by NF-κB activity, via NF-κB-mediated induction of other factors and signaling molecules.

In various cell systems, the transcriptional activity of NFAT5 is critical for cell survival under hyperosmotic conditions [37,38]. Here, we show for the first time that NFAT5 is induced in RPE cells in response to hyperosmotic stress (Figure 9A-E), but not to hypoxia (Figure 9A,C), and that hyperosmolarity increases the DNA binding of the NFAT5 protein (Figure 9F). The gene and protein expression of NFAT5 in RPE cells is tightly regulated by changes in the extracellular osmolarity; up- and downregulation occurred under hyper- and hypoosmotic conditions, respectively (Figure 9A,C). By using pharmacological inhibition and siRNA knockdown of NFAT5, we found that the transcriptional activity of NFAT5 is implicated in the hyperosmotic expression of AQP5 (Figure 10A,F) and production of VEGF (Figure 10B,C,G,H). However, it remains to be determined whether the NFAT5-induced expression of AQP5 and VEGF is a direct or indirect effect via the NFAT5-induced transcriptional regulation of kinases and other enzymes. The data may suggest that NFAT5 represents a key transcription factor that transducts extracellular osmotic changes to the expression of proteins in RPE cells that have functional roles in angiogenesis and edema.

The osmotic conditions at the basal side of the RPE influence the tightness of the outer blood–retinal barrier; i.e., hyperosmolarity decreases and hypoosmolarity increases the tightness of the barrier [17, 21]. Upregulation (Figure 1A-D) and downregulation of VEGF (Figure 1F) under hyper- and

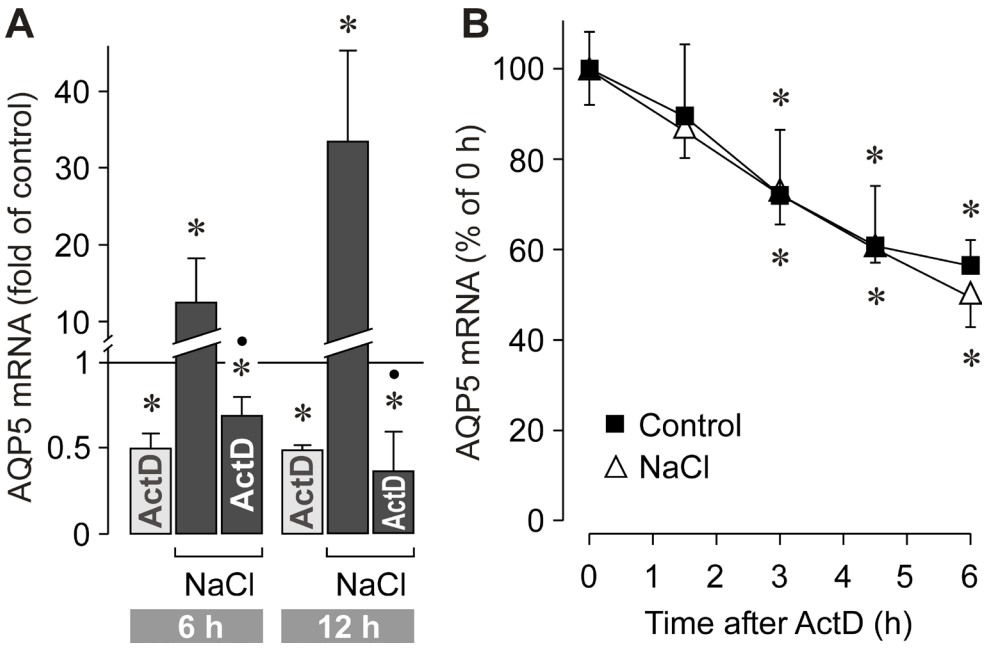

Figure 6. The hyperosmotic upregulation of AQP5 is induced by the stimulation of gene transcription. mRNA expression was determined with real-time RT–PCR analysis. **A.** Inhibition of the RNA polymerase II by actinomycin D (ActD; 5 µg/ml) abrogated the increase in AQP5 mRNA induced by hyperosmotic (+ 100 mM NaCl) medium. The data were obtained after 6 (n=7) and 12 h (n=8) of stimulation, respectively, and are expressed as folds of isoosmotic unstimulated control. Actinomycin D was preincubated for 30 min. **B.** The stability of AQP5 mRNA did not differ between isoosmotic (control; n=4) and hyperosmotic (+ 100 mM NaCl; n=5) conditions. The cells were first treated with iso- and hyperosmotic media for 12 h, followed by the addition of actinomycin D (5 µg/ml). Total RNA was isolated at different time periods after the addition of actinomycin D. Data are means ± SEM obtained in independent experiments performed in triplicate, and are expressed in percentages of 0-h control. Significant difference versus isoosmotic unstimulated control (**A**) and 0 h (**B**): *p<0.05. Significant difference versus NaCl control: ●p<0.05.

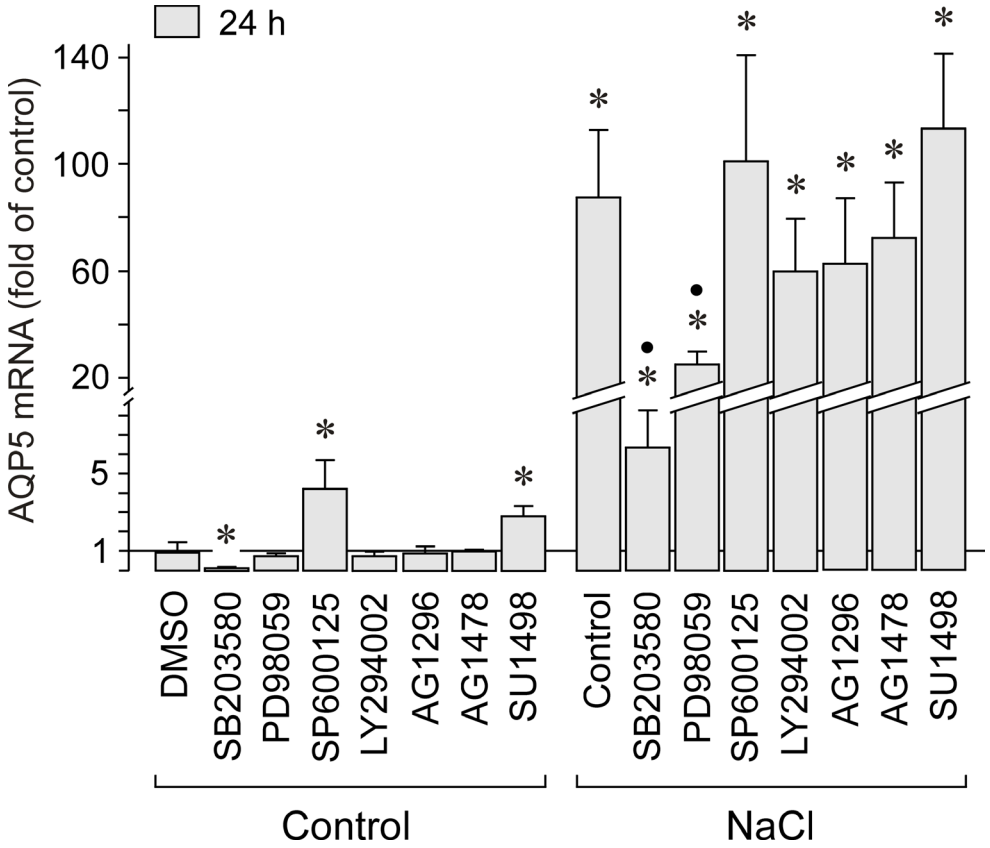

Figure 7. Dependence of the hyperosmotic induction of AQP5 in RPE cells on the activation of signal transduction pathways. The mRNA level was measured with real-time RT–PCR analysis. The cells were cultured for 24 h in isoosmotic (control) and hyperosmotic (+ 100 mM NaCl) media. The hyperosmotic elevation of AQP5 expression was decreased by the inhibitor of p38 MAPK activation, SB203580 (10 µM; n=8), and the inhibitor of ERK1/2 activation, PD98059 (20 µM; n=10), respectively. Inhibitors of JNK activation (SP600125; 10 µM; n=10), of the catalytic subunits of PI3K-related kinases (LY294002; 5 µM; n=8), of the PDGF receptor tyrosine kinase (AG1296; 10 µM; n=8), of the EGF receptor tyrosine kinase (AG1478; 600 nM; n=8), and of the VEGF receptor-2 (SU1498; 10 µM; n=8) did not decrease the hyperosmotic induction of AQP5. The vehicle control was made with DMSO (1%; n=6). Data are means ± SEM obtained in independent experiments performed in triplicate. Significant difference versus isoosmotic unstimulated control: *p<0.05. Significant difference versus NaCl control: ●p<0.05.

hypoosmotic conditions may represent one mechanism by which osmotic changes regulate the tightness of the barrier.

The gene expression of AQP5 was highly increased under hyperosmotic conditions (Figure 5A-C) and decreased under hypoosmotic conditions (Figure 5D). The data may support the assumption that AQP5 is implicated in the resolution of osmotic gradients across the RPE and may facilitate water transport through the RPE, depending on osmotic conditions. In various tissues, AQP5 contributes to the cellular water transport, fluid secretion, and regulation of cellular volume [34, 60, 61]. The hyperosmotic upregulation of AQP5 was shown in the nasal airway epithelium and in lung epithelial cells [35, 55, 62]. Upregulation of AQP5 increases the water permeability of airway epithelia [35], and downregulation of AQP5 reduces lung water transport [36]. Whether alterations in AQP5 expression regulates the water permeability of the RPE remains to be determined. In situ, the hypoosmotic downregulation of AQP5 may decrease the water permeability of RPE cells and thus may inhibit osmotic water flux from the blood into the outer retina. The hyperosmotic upregulation of AQP5 may increase water transport across the RPE. This allows a more efficient resolution of retinal edema when increased extracellular osmolarity, e.g., after high intake of dietary salt [12], induces a breakdown of the blood–retinal barrier [17, 21]. However, the hyperosmotic upregulation of AQP5 might be counterregulated by hypoxia and serum (Figure 5E); this will impair the retinal fluid clearance after the breakdown of the outer blood–retinal barrier, and will contribute to edema development under hypoxic conditions.

It was shown that triamcinolone acetonide decreases the hypoxic gene expression of VEGF [63]. Here, we show that triamcinolone inhibits the hyperosmotic expression of VEGF (Figure 1A), but not of AQP5 (Figure 5F), and abrogates the hyperosmotic secretion of VEGF (Figure 1B). Both the inhibitory effect on the production of VEGF and the ineffectiveness on the expression of AQP5 may support the resolution of retinal edema in situ.

High salt intake results in increased extracellular osmolarity [12]. The present data suggest that one mechanism by which high extracellular NaCl and osmolarity may aggravate the development of neovascular retinal diseases such as

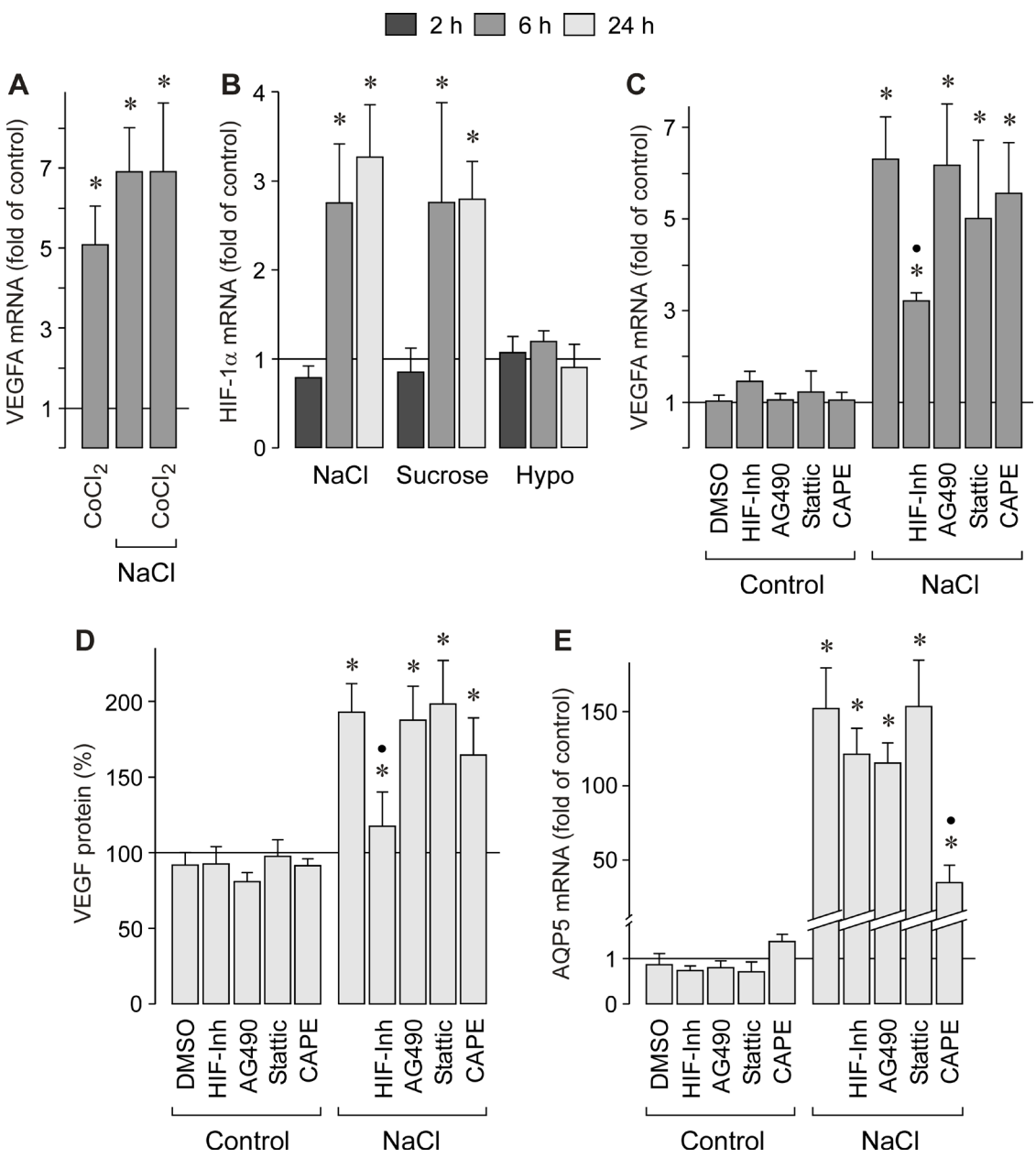

Figure 8. The hyperosmotic induction of VEGF, but not of AQP5, depends in part on the activity of HIF-1. mRNA levels (**A-C, E**) were determined with real-time RT–PCR analysis in cells stimulated for 2, 6, and 24 h, and are expressed as folds of isoosmotic unstimulated control. The level of VEGF-A_{165} protein (**D**) was determined with ELISA in the cultured media of cells stimulated for 24 h, and is expressed in percentages of isoosmotic unstimulated control (100%, corresponding to 383.0±51.1 pg/ml VEGF). **A.** Effects of chemical hypoxia (150 µM $CoCl_2$) and hyperosmotic medium (+ 100 mM NaCl) on the level of VEGF mRNA (n=6). **B.** Relative HIF-1α gene expression level in cells treated with hyperosmotic (+ 100 mM NaCl [n=8] and 100 mM sucrose [n=6], respectively) and hypoosmotic (Hypo; 60% osmolarity) media (n=6). **C.** The hyperosmotic (+ 100 mM NaCl) upregulation of *VEGFA* was decreased in the presence of an HIF inhibitor (HIF-Inh; 5 µM; n=7). The JAK2 inhibitor AG490 (10 µM; n=5), the STAT3 inhibitor Stattic (1 µM; n=7), and the NF-κB inhibitor caffeic acid phenethyl ester (CAPE; 1 µg/ml; n=7) had no significant effects. **D.** The hyperosmotic secretion of VEGF was inhibited by the HIF inhibitor (HIF-Inh; 5 µM; n=6), but not by AG490 (10 µM; n=6), Stattic (1 µM; n=6), or caffeic acid phenethyl ester (CAPE; 1 µg/ml; n=6). **E.** Effects of the HIF inhibitor (HIF-Inh; 5 µM; n=6), AG490 (10 µM; n=6), Stattic (1 µM; n=6), and the NF-κB inhibitor caffeic acid phenethyl ester (CAPE; 1 µg/ml; n=6) on the gene expression of AQP5. Vehicle controls were made with DMSO (1%; n=3 each). Data are means ± SEM obtained in independent experiments performed in triplicate. Significant difference versus isoosmotic unstimulated control: *p<0.05. Significant difference versus NaCl control: ●p<0.05.

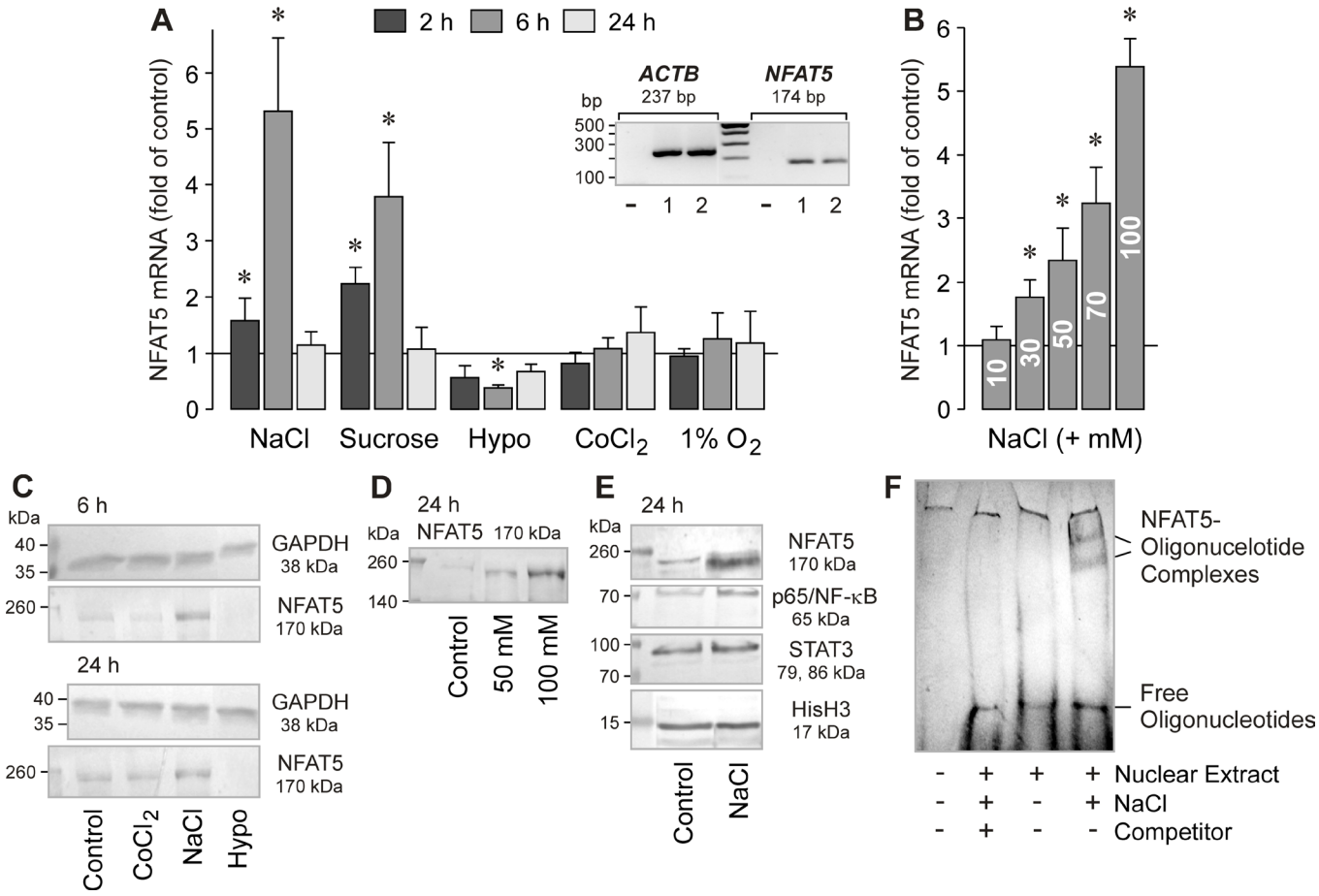

Figure 9. Hyperosmolarity induces NFAT5 gene and protein expression, and the DNA binding of NFAT5, in RPE cells. The mRNA level (**A, B**) was determined with real-time RT–PCR analysis in cells stimulated for 2, 6, and 24 h, and are expressed as folds of isoosmotic unstimulated control. The protein levels (**C-E**) were determined by western blot analysis of cytosolic (**C**) and nuclear extracts (**D, E**) of cells stimulated for 6 and 24 h, respectively. **A.** Effects of osmolarity changes, $CoCl_2$ (150 µM; n=5), and cell culture in 1% O_2 (n=4) on the level of NFAT5 mRNA. The hyperosmotic media were made up by adding 100 mM NaCl (n=5) and 100 mM sucrose (n=3), respectively. The hypoosmotic medium contained 60% of control osmolarity (n=5). *Inset:* Expression of β-actin and NFAT5 genes in RPE cells from different donors (1, 2) determined by RT–PCR. Negative controls (-) were done by adding double-distilled water instead of cDNA as a template. **B.** Dose-dependent effect of high extracellular NaCl on the cellular level of AQP5 mRNA (n=4). The cells were cultured for 6 h in media that were made hyperosmotic by the addition of 10 to 100 mM NaCl. **C.** Effects of $CoCl_2$ (150 µM), as well as of hyperosmotic (+ 100 mM NaCl) and hypoosmotic (Hypo) media, on the cellular level of the NFAT5 protein. Similar results were obtained in three independent experiments using cells from different donors. **D.** Hyperosmolarity (+ 50 and + 100 mM NaCl, respectively) increased dose-dependently the nuclear level of the NFAT5 protein. **E.** Hyperosmolarity (+ 100 mM NaCl) increased the nuclear levels of NFAT5 and p65/NF-κB proteins of RPE cells, while the nuclear level of STAT3 protein remained unchanged. As a control, the nuclear level of the histone H3 (HisH3) protein was determined. **F.** Hyperosmolarity (+ 100 mM NaCl) induces the DNA binding of NFAT5, as indicated by the appearance of complexes of NFAT5 protein and labeled oligonucleotides in EMSA that were not observed under isoosmotic conditions. An excess of unlabeled oligonucleotides (Competitor) abrogated the binding of NFAT5 protein to labeled oligonucleotides. Similar results were obtained in three independent experiments using cells from different donors. Bars represent means ± SEM obtained in independent experiments performed in triplicate. Significant difference versus isoosmotic unstimulated control: *p<0.05.

AMD is a direct effect on RPE cells, via the induction of VEGF production. The finding that chemical hypoxia and extracellular hyperosmolarity induce the gene expression of VEGF in a non-additive fashion (Figure 8A) may suggest that high salt intake may facilitate neovascularization and edema also under normoxic conditions. Because the effects of high extracellular NaCl may occur independently of hypertension, both blood pressure and salt intake should be monitored in patients with neovascular retinal diseases. Because high NaCl induces the transient upregulation of VEGF (Figure 1A), repetitive salt-induced increases in extracellular osmolarity, e.g., during postprandial phases, will have greater effects than

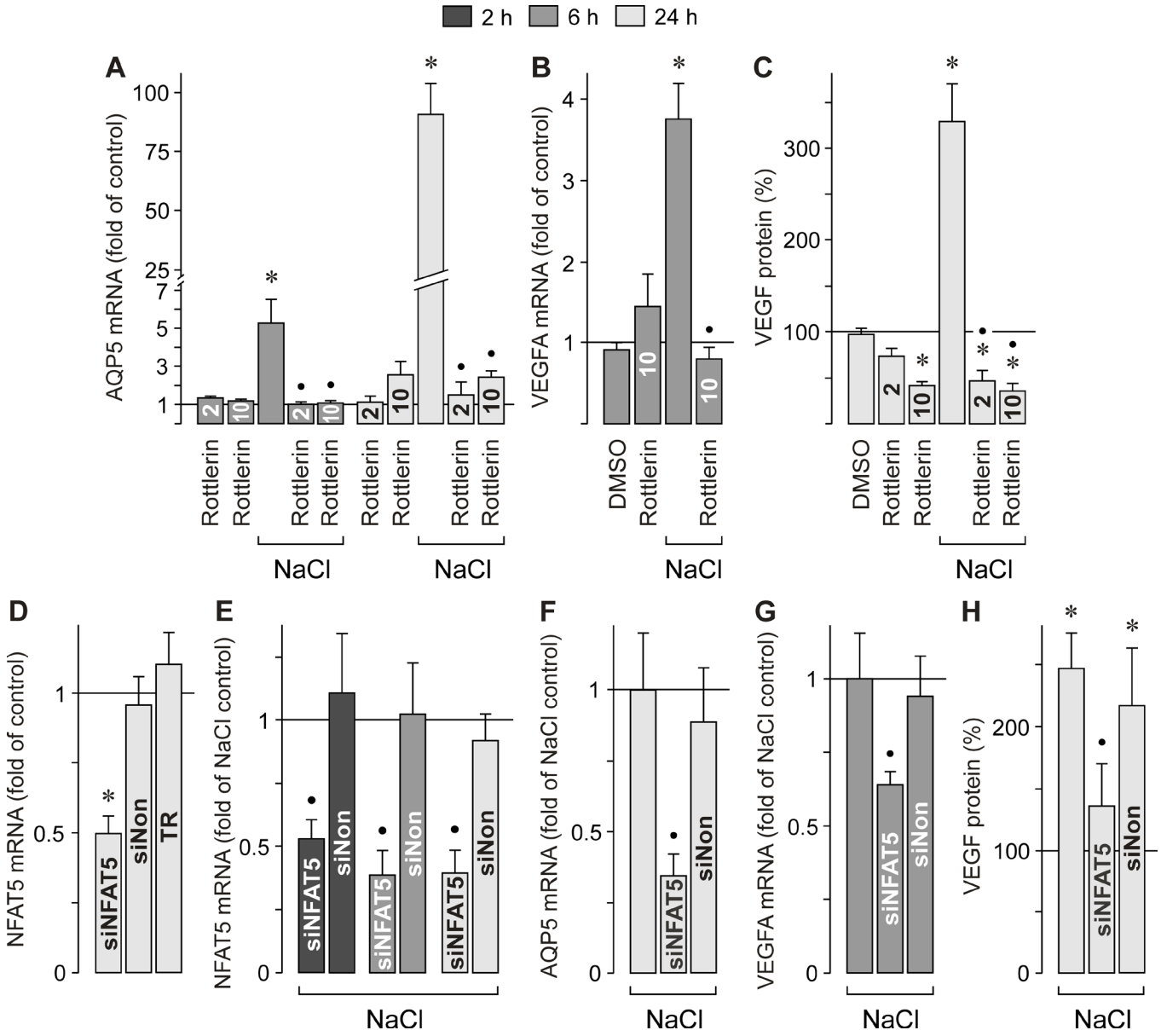

Figure 10. The hyperosmotic induction of AQP5 and VEGF depends on the activity of NFAT5. The mRNA levels (**A, B, D-G**) were determined with real-time RT–PCR analysis in cells stimulated for 2, 6, and 24 h, and are expressed as folds of isoosmotic unstimulated control (**A, B, D**) and NaCl control (**E-G**), respectively. The level of VEGF-A_{165} protein (**C, H**) was determined with ELISA in the cultured media of cells stimulated for 24 h, and is expressed in a percentage of isoosmotic unstimulated control (100%, corresponding to 429.5±71.4 pg/ml [**C**] and 324.2±35.1 pg/ml VEGF [**H**], respectively). **A-C.** The NFAT5 inhibitor rottlerin (2 and 10 µM, respectively) inhibits the hyperosmotic gene expression of AQP5 (**A**; n=7) and VEGF (**B**; n=3), as well as the hyperosmotic secretion of VEGF (**C**; n=5) from RPE cells. Hyperosmolarity was achieved by the addition of 100 mM NaCl to the culture medium. Vehicle control was made with DMSO (1%). **D, E.** Transfection of RPE cells with NFAT5 siRNA (siNFAT5; 5 nM) results in a reduction of the NFAT5 mRNA level in RPE cells cultured in isoosmotic (**D**; n=5) and hyperosmotic (+ 100 mM NaCl) media (**E**; n=3). Data shown in (**D**) were obtained 48 h after siRNA transfection. Thereafter, the cells were stimulated with a hyperosmotic medium for 2, 6, and 24 h, respectively (**E**). As negative controls, nontargeted siRNA (siNon; 5 nM) and a transfection reagent (TR) without siRNA were used. **F, G.** Knocking down the gene expression of NFAT5 with siRNA (siNFAT5; 5 nM) reduced the levels of AQP5 (**F**; n=6) and VEGF mRNAs (**G**; n=6) in cells cultured for 24 (**F**) and 6 h (**G**), respectively, in hyperosmotic (+ 100 mM NaCl) medium. As a negative control, nontargeted siRNA (siNon; 5 nM) was used (n=6 each). **H.** NFAT5 siRNA also reduced the secretion of VEGF induced by hyperosmotic (+ 100 mM NaCl) medium (n=6). Data are means ± SEM obtained in independent experiments performed in triplicate. Significant difference versus isoosmotic unstimulated control: *p<0.05. Significant difference versus NaCl control: ●p<0.05.

a persistent elevation of the extracellular NaCl level. This supports the assumption that reducing the ingestion of dietary salt may have greater protective effects than antihypertensive medications when high salt intake is continued. The finding that hyperosmolarity and the alteration in the transmembrane NaCl gradient induce the upregulation of VEGF in RPE cells independently of hypertension could, at least in part, explain the observation that, although systemic hypertension increases the risk of neovascular AMD [6, 7], antihypertensive medications do not affect the risk of disease [8].

ACKNOWLEDGMENTS

The authors thank Ute Weinbrecht for excellent technical assistance. This study was supported by grants from the Deutsche Forschungsgemeinschaft (KO 1547/7–1 to L.K; GRK 1097/1, RE 849/16–1, to A.R.) and the Geschwister Freter Stiftung (Hannover, Germany).

REFERENCES

1. Wong TY, Mitchell P. The eye in hypertension. Lancet 2007; 369:425-35. [PMID: 17276782].
2. Kostraba JN, Klein R, Dorman JS, Becker DJ, Drash AL, Maser RE, Orchard TJ. The epidemiology of diabetes complications study. IV. Correlates of diabetic background and proliferative retinopathy. Am J Epidemiol 1991; 133:381-91. [PMID: 1994702].
3. Klein R, Klein BE, Moss SE, Cruickshanks KJ. The Wisconsin Epidemiologic Study of Diabetic Retinopathy: XVII. The 14-year incidence and progression of diabetic retinopathy and associated risk factors in type 1 diabetes. Ophthalmology 1998; 105:1801-15. [PMID: 9787347].
4. . UK Prospective Diabetes Study Group. Tight blood pressure control and risk of macrovascular and microvascular complications in type 2 diabetes: UKPDS 38. BMJ 1998; 317:703-13. [PMID: 9732337].
5. Adler AI, Stratton IM, Neil HA, Yudkin JS, Matthews DR, Cull CA, Wright AD, Turner RC, Holman RR. Association of systolic blood pressure with macrovascular and microvascular complications of type 2 diabetes (UKPDS 36): prospective observational study. BMJ 2000; 321:412-9. [PMID: 10938049].
6. Hyman L, Schachat AP, He Q, Leske MC. Hypertension, cardiovascular disease, and age-related macular degeneration. Age-Related Macular Degeneration Risk Factors Study Group. Arch Ophthalmol 2000; 118:351-8. [PMID: 10721957].
7. Klein R, Klein BE, Tomany SC, Cruickshanks KJ. The association of cardiovascular disease with the long-term incidence of age-related maculopathy: the Beaver Dam Eye Study. Ophthalmology 2003; 110:1273-80. [PMID: 12799274].
8. Van Leeuwen R, Tomany SC, Wang JJ, Klein R, Mitchell P, Hofman A, Klein BE, Vingerling JR, Cumming RG, de Jong PT. Is medication use associated with the incidence of early age-related maculopathy? Pooled findings from 3 continents. Ophthalmology 2004; 111:1169-75. [PMID: 15177967].
9. Suzuma I, Hata Y, Clermont A, Pokras F, Rook SL, Suzuma K, Feener EP, Aiello LP. Cyclic stretch and hypertension induce retinal expression of vascular endothelial growth factor and vascular endothelial growth factor receptor-2: potential mechanisms for exacerbation of diabetic retinopathy by hypertension. Diabetes 2001; 50:444-54. [PMID: 11272159].
10. Seko Y, Seko Y, Fujikura H, Pang J, Tokoro T, Shimokawa H. Induction of vascular endothelial growth factor after application of mechanical stress to retinal pigment epithelium of the rat *in vitro*. Invest Ophthalmol Vis Sci 1999; 40:3287-91. [PMID: 10586955].
11. Miller JW, Le Couter J, Strauss EC, Ferrara N. Vascular endothelial growth factor A in intraocular vascular disease. Ophthalmology 2013; 120:106-14. [PMID: 23031671].
12. Lifton RP, Gharavi AG, Geller DS. Molecular mechanisms of human hypertension. Cell 2001; 104:545-56. [PMID: 11239411].
13. Khaw KT, Barrett-Connor E. The association between blood pressure, age and dietary sodium and potassium: a population study. Circulation 1988; 77:53-61. [PMID: 3257173].
14. Qin Y, Xu G, Fan J, Witt RE, Da C. High-salt loading exacerbates increased retinal content of aquaporins AQP1 and AQP4 in rats with diabetic retinopathy. Exp Eye Res 2009; 89:741-7. [PMID: 19596320].
15. Kawasaka K, Yanagida T, Yamamoto S, Yonemura D. Decrease of electrooculographic potential under osmotic stress in man. Jpn J Ophthalmol 1977; 31:23-8. .
16. Steinberg RH, Linsenmeier RA, Griff ER. Retinal pigment epithelial cell contributions to the electroretinogram and electrooculogram. Prog Retinal Res 1985; 4:33-66. .
17. Shirao Y, Steinberg RH. Mechanisms of effects of small hyperosmotic gradients on the chick RPE. Invest Ophthalmol Vis Sci 1987; 28:2015-25. [PMID: 3679749].
18. Winkler BS. Hyperosmolarity and electroretinogram (ERG) potentials in isolated rat retinas: possible implications in diabetic models. Exp Eye Res 2003; 77:115-6. [PMID: 12823995].
19. Gilcrease MZ, Hoover RL. Neutrophil adhesion to endothelium following hyperosmolar insult. Diabetes Res 1991; 16:149-57. [PMID: 1802480].
20. Joussen AM, Murata T, Tsujikawa A, Kirchhof B, Bursell SE, Adamis AP. Leukocyte-mediated endothelial cell injury and death in the diabetic retina. Am J Pathol 2001; 158:147-52. [PMID: 11141487].
21. Orgül S, Reuter U, Kain HL. Osmotic stress in an *in vitro* model of the outer blood-retinal barrier. Ger J Ophthalmol 1993; 2:436-43. [PMID: 8312831].
22. Millay RH, Klein ML, Shults WT, Dahlborg SA, Neuwelt EA. Maculopathy associated with combination chemotherapy

and osmotic opening of the blood-brain barrier. Am J Ophthalmol 1986; 102:626-32. [PMID: 3096140].

23. Bresnick GH. Diabetic maculopathy. A critical review highlighting diffuse macular edema. Ophthalmology 1983; 90:1301-17. [PMID: 6664669].

24. Bressler NM, Bressler SB, Fine SL. 2001. Neovascular (exudative) age-related macular degeneration. In: Schachat AP (ed) *Retina*. Mosby, St Louis, 2001; 1100–35.

25. Strauss O. The retinal pigment epithelium in visual function. Physiol Rev 2005; 85:845-81. [PMID: 15987797].

26. Bringmann A, Pannicke T, Grosche J, Francke M, Wiedemann P, Skatchkov SN, Osborne NN, Reichenbach A. Müller cells in the healthy and diseased retina. Prog Retin Eye Res 2006; 25:397-424. [PMID: 16839797].

27. Stamer WD, Bok D, Hu J, Jaffe GJ, McKay BS. Aquaporin-1 channels in human retinal pigment epithelium: role in transepithelial water movement. Invest Ophthalmol Vis Sci 2003; 44:2803-8. [PMID: 12766090].

28. Nagelhus EA, Mathiisen TM, Ottersen OP. Aquaporin-4 in the central nervous system: cellular and subcellular distribution and coexpression with Kir4.1. Neuroscience 2004; 129:905-13. [PMID: 15561407].

29. Bringmann A, Reichenbach A, Wiedemann P. Pathomechanisms of cystoid macular edema. Ophthalmic Res 2004; 36:241-9. [PMID: 15583429].

30. Verkman AS, Ruiz-Ederra J, Levin MH. Functions of aquaporins in the eye. Prog Retin Eye Res 2008; 27:420-33. [PMID: 18501660].

31. Hollborn M, Rehak M, Iandiev I, Pannicke T, Ulbricht E, Reichenbach A, Wiedemann P, Bringmann A, Kohen L. Transcriptional regulation of aquaporins in the ischemic rat retina: upregulation of aquaporin-9. Curr Eye Res 2012; 37:524-31. [PMID: 22577771].

32. Molinas SM, Trumper L, Marinelli RA. Mitochondrial aquaporin-8 in renal proximal tubule cells: evidence for a role in the response to metabolic acidosis. Am J Physiol Renal Physiol 2012; 303:F458-66. [PMID: 22622463].

33. Calamita G, Ferri D, Gena P, Liquori GE, Cavalier A, Thomas D, Svelto M. The inner mitochondrial membrane has aquaporin-8 water channels and is highly permeable to water. J Biol Chem 2005; 280:17149-53. [PMID: 15749715].

34. Ma T, Fukuda N, Song Y, Matthay MA, Verkman AS. Lung fluid transport in aquaporin-5 knockout mice. J Clin Invest 2000; 105:93-100. [PMID: 10619865].

35. Pedersen PS, Braunstein TH, Jørgensen A, Larsen PL, Holstein-Rathlou NH, Frederiksen O. Stimulation of aquaporin-5 and transepithelial water permeability in human airway epithelium by hyperosmotic stress. Pflugers Arch 2007; 453:777-85. [PMID: 17043812].

36. Zhang YW, Bi LT, Hou SP, Zhao XL, Song YL, Ma TH. Reduced lung water transport rate associated with downregulation of aquaporin-1 and aquaporin-5 in aged mice. Clin Exp Pharmacol Physiol 2009; 36:734-8. [PMID: 19215235].

37. Woo SK, Lee SD, Kwon HM. TonEBP transcriptional activator in the cellular response to increased osmolality. Pflugers Arch 2002; 444:579-85. [PMID: 12194010].

38. Ho SN. The role of NFAT5/TonEBP in establishing an optimal intracellular environment. Arch Biochem Biophys 2003; 413:151-7. [PMID: 12729611].

39. Chen R, Hollborn M, Grosche A, Reichenbach A, Wiedemann P, Bringmann A, Kohen L. Effects of the vegetable polyphenols EGCG, luteolin, apigenin, myricetin, quercetin, and cyanidin in retinal pigment epithelial cells. Mol Vis 2014; 20:242-58. [PMID: 24623967].

40. Fraser-Bell S, Kaines A, Hykin PG. Update on treatments for diabetic macular edema. Curr Opin Ophthalmol 2008; 19:185-9. [PMID: 18408491].

41. Matsuda S, Gomi F, Oshima Y, Tohyama M, Tano Y. Vascular endothelial growth factor reduced and connective tissue growth factor induced by triamcinolone in ARPE19 cells under oxidative stress. Invest Ophthalmol Vis Sci 2005; 46:1062-8. [PMID: 15728566].

42. Arsenijevic T, Vujovic A, Libert F, Op de Beeck A, Hébrant A, Janssens S, Grégoire F, Lefort A, Bolaky N, Perret J, Caspers L, Willermain F, Delporte C. Hyperosmotic stress induces cell cycle arrest in retinal pigmented epithelial cells. Cell Death Dis 2013; 4:e662-[PMID: 23744362].

43. Hollborn M, Ulbricht E, Reichenbach A, Wiedemann P, Bringmann A, Kohen L. Transcriptional regulation of aquaporin-3 in human retinal pigment epithelial cells. Mol Biol Rep 2012; 39:7949-56. [PMID: 22535323].

44. An WG, Kanekal M, Simon MC, Maltepe E, Blagosklonny MV, Neckers LM. Stabilization of wild-type p53 by hypoxia-inducible factor 1α. Nature 1998; 392:405-8. [PMID: 9537326].

45. Forsythe JA, Jiang BH, Iyer NV, Agani F, Leung SW, Koos RD, Semenza GL. Activation of vascular endothelial growth factor gene transcription by hypoxia-inducible factor 1. Mol Cell Biol 1996; 16:4604-13. [PMID: 8756616].

46. Niu G, Wright KL, Huang M, Song L, Haura E, Turkson J, Zhang S, Wang T, Sinibaldi D, Coppola D, Heller R, Ellis LM, Karras J, Bromberg J, Pardoll D, Jove R, Yu H. Constitutive Stat3 activity up-regulates VEGF expression and tumor angiogenesis. Oncogene 2002; 21:2000-8. [PMID: 11960372].

47. Lee K, Lee JH, Boovanahalli SK, Jin Y, Lee M, Jin X, Kim JH, Hong YS, Lee JJ. (Aryloxyacetylamino)benzoic acid analogues: a new class of hypoxia-inducible factor-1 inhibitors. J Med Chem 2007; 50:1675-84. [PMID: 17328532].

48. Meydan N, Grunberger T, Dadi H, Shahar M, Arpaia E, Lapidot Z, Leeder JS, Freedman M, Cohen A, Gazit A, Levitzki A, Roifman CM. Inhibition of acute lymphoblastic leukaemia by a Jak-2 inhibitor. Nature 1996; 379:645-8. [PMID: 8628398].

49. Schust J, Sperl B, Hollis A, Mayer TU, Berg T. Stattic: a small-molecule inhibitor of STAT3 activation and dimerization. Chem Biol 2006; 13:1235-42. [PMID: 17114005].

50. Natarajan K, Singh S, Burke TR Jr, Grunberger D, Aggarwal BB. Caffeic acid phenethyl ester is a potent and specific inhibitor of activation of nuclear transcription factor NF-κB. Proc Natl Acad Sci USA 1996; 93:9090-5. [PMID: 8799159].

51. Zhao H, Tian W, Cohen DM. Rottlerin inhibits tonicity-dependent expression and action of TonEBP in a PKCδ-independent fashion. Am J Physiol Renal Physiol 2002; 282:F710-7. [PMID: 11880333].

52. Tran TL, Bek T, Holm L, La Cour M, Nielsen S, Prause JU, Rojek A, Hamann S, Heegaard S. Aquaporins 6–12 in the human eye. Acta Ophthalmol (Copenh) 2013; 91:557-63. [PMID: 22974000].

53. Kawedia JD, Yang F, Sartor MA, Gozal D, Czyzyk-Krzeska M, Menon AG. Hypoxia and hypoxia mimetics decrease aquaporin 5 (AQP5) expression through both hypoxia inducible factor-1α and proteasome-mediated pathways. PLoS ONE 2013; 8:e57541-[PMID: 23469202].

54. Richard DE, Berra E, Gothié E, Roux D, Pouysségur J. p42/p44 mitogen-activated protein kinases phosphorylate hypoxia-inducible factor 1α (HIF-1α) and enhance the transcriptional activity of HIF-1. J Biol Chem 1999; 274:32631-7. [PMID: 10551817].

55. Laughner E, Taghavi P, Chiles K, Mahon PC, Semenza GL. HER2 (neu) signaling increases the rate of hypoxia-inducible factor 1α (HIF-1α) synthesis: novel mechanism for HIF-1-mediated vascular endothelial growth factor expression. Mol Cell Biol 2001; 21:3995-4004. [PMID: 11359907].

56. Zhou B, Ann DK, Li X, Kim KJ, Lin H, Minoo P, Crandall ED, Borok Z. Hypertonic induction of aquaporin-5: novel role of hypoxia-inducible factor-1α. Am J Physiol Cell Physiol 2007; 292:C1280-90. [PMID: 17108010].

57. Lukiw WJ, Ottlecz A, Lambrou G, Grueninger M, Finley J, Thompson HW, Bazan NG. Coordinate activation of HIF-1 and NF-κB DNA binding and COX-2 and VEGF expression in retinal cells by hypoxia. Invest Ophthalmol Vis Sci 2003; 44:4163-70. [PMID: 14507857].

58. Towne JE, Krane CM, Bachurski CJ, Menon AG. Tumor necrosis factor-α inhibits aquaporin 5 expression in mouse lung epithelial cells. J Biol Chem 2001; 276:18657-64. [PMID: 11279049].

59. Yao C, Purwanti N, Karabasil MR, Azlina A, Javkhlan P, Hasegawa T, Akamatsu T, Hosoi T, Ozawa K, Hosoi K. Potential down-regulation of salivary gland AQP5 by LPS via cross-coupling of NF-κB and p-c-Jun/c-Fos. Am J Pathol 2010; 177:724-34. [PMID: 20522648].

60. Funaki H, Yamamoto T, Koyama Y, Kondo D, Yaoita E, Kawasaki K, Kobayashi H, Sawaguchi S, Abe H, Kihara I. Localization and expression of AQP5 in cornea, serous salivary glands, and pulmonary epithelial cells. Am J Physiol 1998; 275:C1151-7. [PMID: 9755069].

61. Levin MH, Verkman AS. Aquaporin-dependent water permeation at the mouse ocular surface: *in vivo* microfluorimetric measurements in cornea and conjunctiva. Invest Ophthalmol Vis Sci 2004; 45:4423-32. [PMID: 15557451].

62. Hoffert JD, Leitch V, Agre P, King LS. Hypertonic induction of aquaporin-5 expression through an ERK-dependent pathway. J Biol Chem 2000; 275:9070-7. [PMID: 10722758].

63. Sears JE, Hoppe G. Triamcinolone acetonide destabilizes VEGF mRNA in Müller cells under continuous cobalt stimulation. Invest Ophthalmol Vis Sci 2005; 46:4336-41. [PMID: 16249516].

Articles are provided courtesy of Emory University and the Zhongshan Ophthalmic Center, Sun Yat-sen University, P.R. China. The print version of this article was created on 9 April 2015. This reflects all typographical corrections and errata to the article through that date. Details of any changes may be found in the online version of the article.